IEEE Access
Multidisciplinary | Rapid Review | Open Access Journal

Received June 4, 2020, accepted June 7, 2020, date of publication June 18, 2020, date of current version June 30, 2020.

Digital Object Identifier 10.1109/ACCESS.2020.3003273

A W-Band 3-D Integrated Mini-SAR System With High Imaging Resolution on UAV Platform

MAN-LAI DING, CHI-BIAO DING, LI TANG, XUE-MEI WANG, JIA-MENG QU, AND RUI WU
National Key Laboratory of Microwave Imaging Technology, Aerospace Information Research Institute, Chinese Academy of Sciences, Beijing 621000, China
Corresponding author: Chi-Biao Ding (cbding@mail.ie.ac.cn)

This work was supported by the National Key Basic Research Program of China under Grant 2019YFA0210204.

ABSTRACT The light-small multi-rotor unmanned aerial vehicle (UAV) carrying with a mini synthetic aperture radar (SAR) payload has provided an advanced information acquisition technology for the target detecting and imaging fields. In this paper, a W-band compact SAR system is proposed, which has been successfully deployed on the unmanned aerial vehicle (UAV) platform demonstrating state-of-the-art imaging resolution of about 4.5 cm. In order to achieve remarkable compactness, light weight and power-saving feature for the proposed system, the techniques of the three-dimensional (3-D) integration are adopted, where a whole-system size of only $67 \times 60 \times 50$ mm^3 and the weight of 400 g are obtained. This proposed system achieves higher SAR-imaging resolution thanks to the contributions of many efforts, including the technique of high-linearity waveform generation, the substrate integrated waveguide (SIW) antenna with high isolation by the electromagnetic band-gap (EBG) mechanism, and a novel motion compensation method for the imaging formation. To validate this proposed idea, a UAV SAR prototype operating at W-band is designed and fabricated. The measurements show great signal-to-noise ratio imaging results with excellent focusing effect. The proposed SAR system is promisingly an ideal candidate for the target detecting/imaging applications deployed on the UAV platform.

INDEX TERMS Frequency modulated source, mini synthetic aperture radar (SAR), high imaging resolution, unmanned aerial vehicle (UAV), 3-D integration.

I. INTRODUCTION

UAV-borne radars have aroused great interests not only in the academic communities but also in the industrial applications. This is because as compared with that of the traditional airborne systems, the operation of the multi-rotor UAV is more flexible without assistance of the take-off and landing runways, which facilitates the expedited deployment of the UAV-borne radars in a relatively harsh scenario where changes may happen in the twinkling of an eye. Thus, UAV-borne radars potentially could find the targets much faster than that of the traditional counterparts implying higher detection efficiency. In addition, the size of UAVs, especially the multi-rotor UAVs, is much smaller than that of the traditional aerial vehicles, meaning higher survival rate in the warfare by hiding the UAVs from the radar detection. Therefore, the multi-rotor UAV-borne radar is an efficient platform for the information acquisitions [1].

The associate editor coordinating the review of this manuscript and approving it for publication was Zhongyi Guo.

Synthetic aperture radar (SAR) is a system that moving the radar antenna over a target region to provide finer spatial resolution rather than conventional beam-scanning radars [2]. The synthetic antenna aperture of the SAR could be unlimited large by simply cruising around the selected area, while it is impossible for the traditional beam-scanning radars to obtain the same detection performance by deploying physically large antenna with the same aperture size. The UAV-borne SARs have additionally brought revolutionary influence on the applications of target detection and imaging. Many UAV-borne SARs were developed for scientific and other practical applications, including the high-resolution imaging of ground, tracking of the moving target, environmental monitoring and antenna pattern verification [3]–[6]. Therefore, the development of a UAV-based SAR with miniaturized size and high resolution is of particular worth for remote sensing applications.

Different from those of the traditional UAV SARs, there exist many limitations and technical challenges for the multi-rotor UAV SARs, such as size reduction of

SAR payloads, power-saving techniques for broader cruising range, thermal management of electronics, imaging algorithm for the motion compensation and defocusing issues, *etc*. To tackle these issues, many efforts have been made and introduced for the terrain monitoring and observation applications. For example, the polarimetric radar ARBRES-X SAR working on X-band mounted on a UAV for imaging applications is proposed [7]. Although the aluminum bar together with the patch antennas was used to lighten the weight, every module cannot be integrated that lead to a large volume. Besides, there is a defocusing problem in the retrieved images due to the platform deviation from the nominal trajectory and the flight instabilities [8]. As has been discussed in [9]–[14], the SAR systems working on the millimeter waves like W-band can obtain the detailed ground texture features, the high-resolution and minimal changes of the target benefited from the unique reflection characteristics and broadband characteristics of such millimeter waves. Comparing with the other microwave band, W-band SAR systems have smaller antennas and circuits while maintaining the same performance, which have been the research focus for the light-weight UAV based payloads. Meanwhile, many integrated chips are developed to replace the traditional circuits and units, which greatly reduce the size of whole SAR system. But the shrink size due to high-density assembly leads to heat concentration, which may degrade the SAR performance [15], [16]. As the operation frequency goes higher, especially in terahertz bands, traditional integration methods (e.g., the connection between flanges for waveguides) have encountered similar size-reduction bottleneck [17]. Therefore, all these traditional solutions still demonstrates limitations and challenges on the size reduction of the SAR payload, and the improvement for imaging resolution.

In our previous work [18], [19], a W-band mini-SAR on multi-rotor UAV platform has been initially evaluated to validate the system performance. This paper further presents such compact W-band drone-borne SAR system in detail to offer new possibilities in observation. Despite the previous state-of-the-art imaging systems at microwaves, this system is fully 3D packaged to obtain the solid-state and miniaturization structure. An analog phase-locked loop (PLL) technology is proposed to achieve the high linearity frequency modulation waveform generation. And then the electromagnetic band-gap (EBG) mechanism is introduced to acquire high isolation without increasing the antennas distance. Combining with the motion compensation method, the high imaging resolution will be achieved based on the above methods.

This paper is organized as follows. In Section II, the implementation and the performance characteristics of the proposed SAR payload are described. Section III illustrates the key technologies to improve the imaging resolutions such as the 3-D integration strategy, the linear frequency modulation waveform generator based on the analog PLL and the high isolation transceiver antennas based on the EBG. To validate the proposed idea, in Section IV, the measurement set up is demonstrated with the high-resolution imaging results.

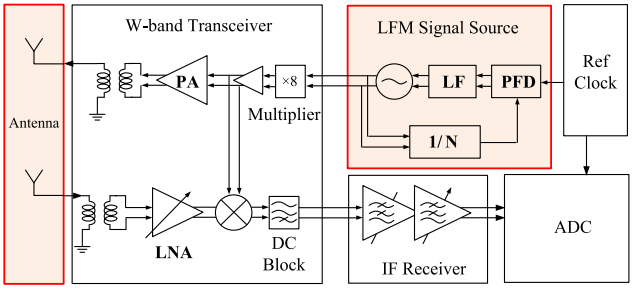

FIGURE 1. Schematic view of the proposed W-band UAV mini-SAR system.

Comparisons between the proposed UAV SAR and the traditional UAV SAR manifesting that the proposed SAR is promisingly an ideal candidate for the applications of UAV high-resolution imaging. Finally, this paper is concluded in Section V.

II. W-BAND SAR SYSTEM SCHEME

A. MINI-SAR ARCHITECTURE

Traditional micro-SAR design architecture include DAC/DDS, up-converter, clock and other modules, in which the schematic structure is complex with high power consumption and serious deterioration of performance with chip integrating. In this section, a different design scheme is proposed to realize the miniature SAR system on the multi-rotor UAV platform. The proposed SAR system design scheme is shown in Fig.1. This micro-SAR consists of a reference clock, a linear frequency modulation (LFM) source, a millimeter-wave transceiver front end, two antennas, an intermediate frequency (IF) channel, and an analog-to-digital converter (ADC). The classical frequency modulation continuous wave (FMCW) system is adopted in this SAR. The de-frequency modulation system is employed for the received radar echo signal to reduce the IF effectively. In addition, the sampling and quantization of the echo signal can be easily realized by using low-speed ADC in this system, which can greatly reduce the amount of data for signal processing. Compared with that of the traditional micro-SAR scheme, this reference clock is also simplified greatly, which only needs a low frequency referenced signal for the PLL and ADC modules. For example, a simple 50 MHz fixed frequency crystal oscillator can meet full coherent work requirements of the radar system. Furthermore, a novel LFM signal generation method based on analog PLL technology is used for the system, which can fully utilize the characteristics of a voltage-controlled oscillator (VCO) to directly generate a high-frequency broadband LFM signal. In addition, the narrow-band filtering feature of the PLL can obtain the lower phase noise, good spur suppression and other advantages for this transmit waveform signals. There are still other new methods such as decoupling between transmitting and receiving antennas have also been improved in this system. All the above-mentioned improvement designs make such mini-SAR have the characteristics of simple circuit structure

TABLE 1. Main performance of this proposed mini-SAR system.

Parameter name	*Value*
Carrier frequency	94 GHz
Signal bandwidth	4000 MHz
Modulation mode	LFM
Frequency modulation rate	20 MHz/μs
Max imaging rang	600 m
Look angle	60°
Slant range resolution	3.75 cm
Weight	0.4 kg
Volume	67×60×50 mm^3

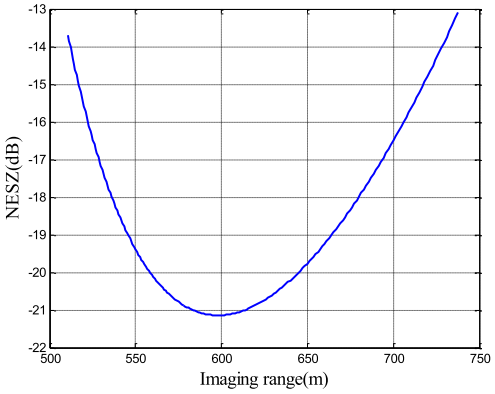

FIGURE 2. Simulation results of NESZ.

and low power consumption, which can also be integrated through three-dimensional feasibly.

B. SYSTEM PERFORMANCE

The main performance characteristics of this miniature SAR system are shown in table 1. Various characteristics including carrier frequency, signal bandwidth, modulation method, resolution and maximum working distance have been made clearly. As is well known that the Noise Equivalent Scattering Coefficient (NESZ) characteristic is the core parameter of SAR imaging quality. Therefore, the NESZ of side-looking strip SAR is firstly designed and demonstrated, which can be expressed as,

$$NESZ = \frac{2 \cdot (4 \times \pi)^3 \cdot r^3 \cdot V_a \cdot k \cdot T}{\lambda^3 \cdot G_t \cdot G_r \cdot P_{av} \cdot \rho_r} k_s \tag{1}$$

In this formula (1), $NESZ$ denotes noise equivalent scattering coefficient, r is the imaging range, V_a is the moving velocity of UAV, k is the Boltzmann constant, T is the equivalent noise temperature of the receiver, λ is the operation wavelength of SAR, G_t and G_r are the gains of transmitting and receiving antennas respectively, P_{av} is the average transmitting power, ρ_r is the system range resolution, k_s is the weighting of system loss and other losses.

According to the equation (1), the NESZ of the SAR system is simulated and analyzed, as shown in Fig. 2. The NESZ is better than −21.0 dB in the 600 m range, which means that the system satisfies the basic condition for high-SNR imaging. In addition, the slant range resolution represented by R_{es} can be derived from fractional bandwidth.

$$R_{es} = \frac{c}{2 \cdot BW} \tag{2}$$

where BW is the signal bandwidth, and c is the light speed. When the beam downward angle of the radar mounted on UAV is θ, the ground resolution can be calculated by the following equation (3).

$$\Delta R = \frac{c}{2 \cdot BW \cdot \sin\theta} \tag{3}$$

Therefore, this SAR system has 4.3 cm ground resolution, when the installation look angle is 60°.

III. KEY TECHNOLOGIES OF THE MINI-SAR SYSTEM

A. 3D INTEGRATION STRATEGY

The millimeter-wave circuits are usually integrated through the traditional two-dimensional planar technology combining with the printed circuit board (PCB) and low temperature co-fired ceramic (LTCC) processes. All the active chips with different functions and peripheral passive devices can be assembled to improve the system integration. Although two-dimensional planar integrating way can reduce the system size, there is still an limitation of integration since the main chips should be mounted on a planar layout properly. Besides, the resistance-capacitance delay and parasitic capacitance caused by the excessively long signal will reduce the operation speed of devices when the chip number is large. As compared with the two-dimensional (2D) integration, the three-dimensional (3D) integration technology is an effective way to achieve the higher integration level, meaning miniaturization, light weight, high density and excellent electrical capability [20]. 3D integration solution can not only fully use the 3D space, reduce the circuit area, shorten the leading wire length and increase the transmission speed, but can also heterogeneously integrate chips based on different processes, such as silicon-based, compound semiconductor, MEMS. It is beneficial to achieve multi-function and larger-scale integration [21], [22].

Therefore, such 3D integration technology is used for this W-band micro-SAR on UAV platform developed in this paper, which effectively improves the system integration. The diagram of this 3D fully integrated SAR system is shown in Figure 3. In this packaged 3D configuration, three-dimensional layers have been carried out firstly according to the function and frequency band. In the proposed integration architectures, the antenna and transmitter/receiver (T/R) layer working in the W band, the frequency synthesis and intermediate frequency layer working in the microwave frequency band, while the digital and power layer working at low frequencies. 3-D integrating with stack way can improve the efficiency of space utilization and obtain high isolation between modules. Secondly, the vertical interconnection method is adopted for the signal connection in different

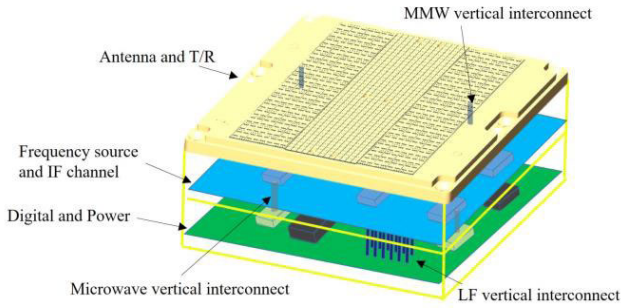

FIGURE 3. The diagram of three-dimensional integrated System.

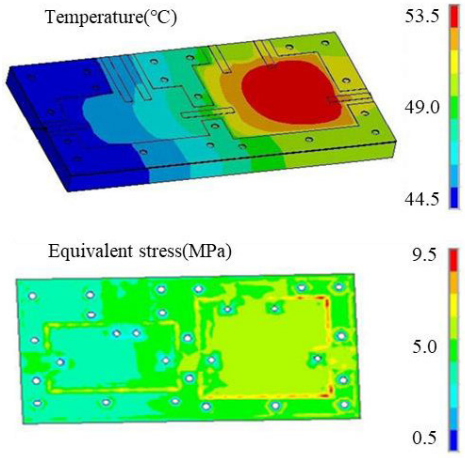

FIGURE 4. Thermal stress simulation of key parts in system.

layers. The vertical transition between the planar millimeter-wave signals and the antenna port is required for the vertical interconnection between the millimeter-wave antenna and T/R chips. The well matching and low-loss transmission can be also achieved from the simulation. At last, the thermal and stress design is the important part for such high-density 3D integrating system, which has been simulated too. The thermal conduction characteristics as well as the structural stress changes from the radio frequency (RF) and high-power chips are analyzed, as shown in Figure 4. The chip layout and signal transmission mode can be following optimized to improve the overall thermal management efficiency and mitigate the risk of thermal stress in the system.

In conclusion of the above design and optimization, a highly integrated W-band micro-SAR principle prototype for mini-UAV is finally developed, with a volume of 67 mm × 60 mm × 50 mm and a weight of only 400 g. Compared with that of the traditional micro-SAR, the volume-to-weight ratio of the proposed SAR has been reduced by more than 5 times. Such highly integrated design will greatly expand the application areas of W-band UAV-based micro-SAR.

B. LFM TECHNOLOGY BASED ON ANALOG PLL

The analog PLL technology is utilized to generate LFM signal, which simplifies the circuit structure and reduces system power consumption greatly. However, the frequency linearity and phase stability between pulses of the LFM signal generated by the analog method will be much poorer than the digital circuit method. The solution to design the high LFM circuit based on the PLL is a urgent technology for the requirement of SAR imaging.

Thus, a new mathematical model of the phase-locked frequency modulation source circuit is proposed and established in this paper. The pulse compression quality and the imaging quality of SAR system will be evaluated through analyzing the output signal. When an active integral loop filter is using for the phase-locked loop, the error transfer function of PLL reference clock and the output signal can be expressed as the formula (4).

$$H_e(s) = \frac{s^2}{s^2 + 2s\xi\omega_n + \omega_n^2} \tag{4}$$

where, $\omega_n = \sqrt{\frac{K_0 K_d}{N\tau_1}}$, $\xi = \frac{\omega_n}{2}\tau_2$, ω_n is the angular frequency, ξ is the damping factor, τ_1 and τ_2 are the time constants of active filters, K_0 is the tuning gain for PLL VCO, K_d is the phase gain and N is the PLL multiple. The LFM signal will present the phase step excitation and LFM excitation when converting between pulses and inside pulse, respectively. The exciting signal can be expressed as formula (5)

$$\theta_i = S_{btwp} + S_{inp} \tag{5}$$

where S_{btwp} is phase step excitation, S_{inp} is the LFM excitation, then θ_i can be expressed as (6).

$$\theta_i = \theta_0 \cdot u(t) + k \cdot \pi \cdot t^2 \cdot u(t) \tag{6}$$

where k (Hz/s) is the rate of frequency modulation, u(t) is the step signal, θ_0 is the phase step. The Laplace transform from equation (6) can be obtained as (7).

$$\Theta(s) = k \cdot \pi \Big/ s^3 + \theta_0 / s \tag{7}$$

Thus the phase error of the PLL in LFM mode will be given as equation (8).

$$\begin{aligned}\Theta(s) &= {}_e(s)\,\Theta(s) \\ &= \frac{s^2}{s^2 + 2s\xi\omega_n + \omega_n^2} \cdot \left(\theta_0 / s + k \cdot \pi \Big/ s^3\right)\end{aligned} \tag{8}$$

According to the inverse Laplace transform of equation (8), the frequency error and phase error of the LFM output signal changing with time can be transformed. The nearly ideal pulse compression results can be acquired through using pulse compression results in the range and azimuth directions of LFM output signal as well as optimizing τ_1, τ_2 and k. The range pulse compression results are shown in Figure 5, and the azimuth pulse compression results are shown in Figure 6.

In conclusion of this above discussion, a mathematical model based on the PLL LFM working mode has been established. The loop parameters have been iteratively optimized by simulating and measuring the PLL. The PLL can work in the tracking lock state during the entire process of generating the LFM signal. The LFM signal of PLL can be collected by

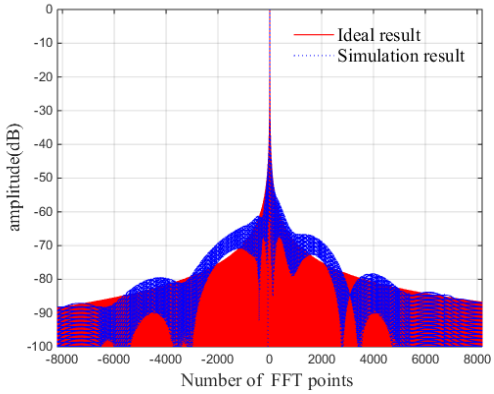

FIGURE 5. The pulse compression results in the range direction.

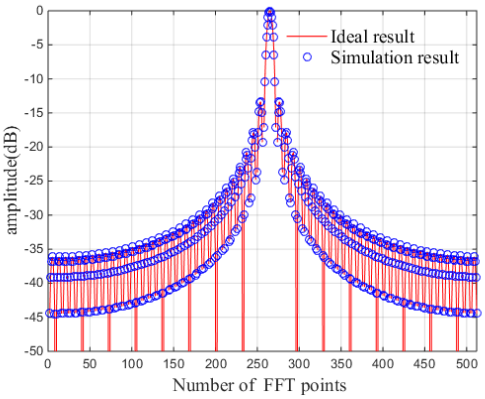

FIGURE 6. The pulse compression results in the azimuth direction.

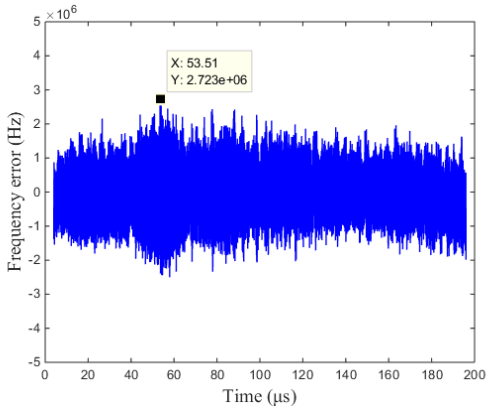

FIGURE 7. Frequency error of The LFM signals generated by the analog PLL.

the high sampling rate oscilloscope, and then the frequency error of the LFM signal can be obtained by the short-time Fourier analysis, as shown in Figure 7. Furthermore, the frequency linearity of the system can be also calculated by equation (9) without considering the influence of frequency multiplier and amplifier. Figure 8 gives this calculated system frequency linearity of about 0.0054. At the same time, the phase between pulses has good stability in the IF signal,

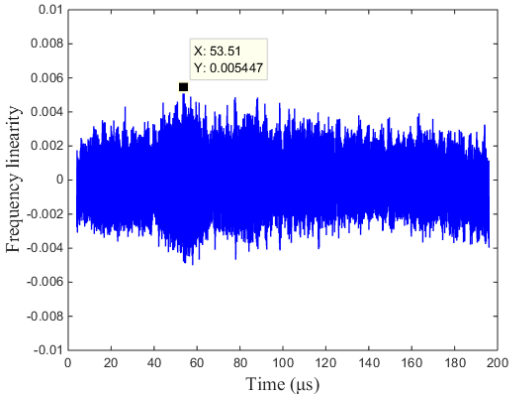

FIGURE 8. Frequency linearity of the system.

which benefits from the de-chirp receiver. Thus, good pulse compression quality in the range and azimuth directions are both obtained.

$$F_{linearity} = f_e / BW \tag{9}$$

where $F_{linearity}$ is the frequency linearity, f_e is the frequency error, BW is the signal bandwidth.

C. HIGH ISOLATION MILLIMETER-WAVE ANTENNAS

Because of the development of the load platform integration and the miniature FMCW SARs, the impact of the signal leakage from transmitting antenna to receiving antenna degrading receiving system performance has been more and more serious. The isolation between the transceiver antennas has become one of the key factors, which poses limitations on the FMCW SAR performance. The signal leakage between the receiving and transmitting antennas is caused by many aspects, in which, the surface-wave crosstalk is one of the important electromagnetic leaking ways, especially in the millimeter-wave frequency band [23]. The traditional simple solution addresses such issues by increasing the distance between two transceiver antennas. The other method is adding an isolation plates to reduce surface waves and space diffraction waves. However, both two approaches are no longer applicable for the currently developed miniature systems due to their large sizes.

An electromagnetic band gap structure (EBG) [24], which can suppress the surface waves between coplanar transceiver antennas, will be adopted to improve the isolation in this W-band mini-SAR on multi-rotor UAV platform. EBG is a low-profile electromagnetic structure, which can be formed by etching process. The periodic metallic structure on the surface of a dielectric substrate can lead to the blocking effect, which is similar to a band-stop filter. Such simple planar integrated EBG structure can suppress surface waves, thereby improve the isolation. Fig. 9 is the proposed W-band transceiver antennas with EBG structures. Fig. 10 shows the isolation comparisons between the antennas with and without EBG construction. The measured results have also been shown in Fig. 10, which shows minor deviation from the

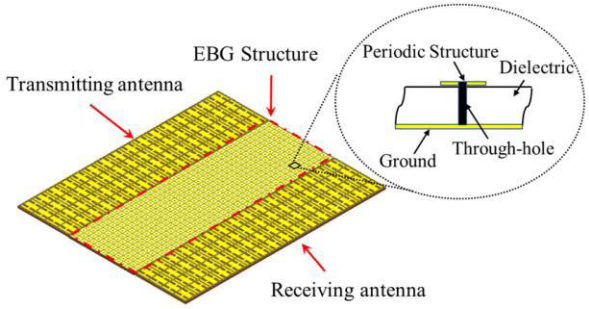

FIGURE 9. W-band transceiver antennas with EBG structures.

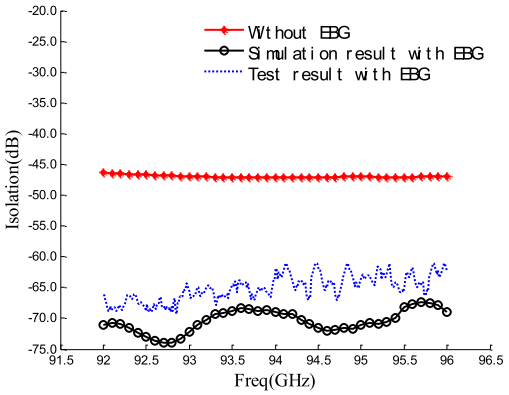

FIGURE 10. The isolation of antennas.

simulated results due to the fabrication errors. The isolation between the transceiver antennas can be improved with 15 dB than that of the one without EBG. Such isolation improvement will increase the SAR resolution.

In addition, the influence of EBG on the beam of antenna is an important problem, which should be considered. It has been found that the EBG will cause the distortion of far-side lobe based on the electromagnetic simulations of antenna radiation patterns. However, the adverse effects including direction deviation and shape distortion on the main beam shape have not been observed obviously. This system generally intercepts the target information within 3dB width of the main beam for imaging, thus the EBG structures will not cause image quality degradation.

D. MOTION COMPENSATION METHOD

There are two particularities for this motion compensation of the W-band UAV-based SAR. Because of the working wavelength of 3 mm is short, the motion errors will be more sensitive. The short-term relative motion measurement accuracy of 0.2 mm should be required. It is difficult to meet such requirements of position and attitude measurement accuracy even if equipping with the current high-precision POS measurement system. Besides, the SAR imaging will be more difficult with the less stable platform due to that the light-small UAV is especially susceptible to atmospheric turbulence. At the same time, this system uses an inertial measurement unit based on micro-electromechanical system

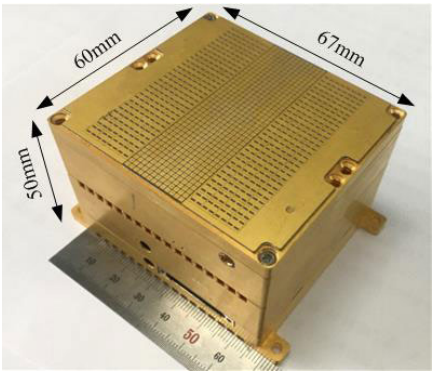

FIGURE 11. W band mini-SAR prototype.

technology (MEMS-IMU) to complete the motion error measurement of the platform in consideration of the cost and weight. But the measurement accuracy of the MEMS-IMU is relatively low, which further increases the SAR imaging difficulty.

Therefore, a motion compensation method based on the signal fusion combining MEMS-IMU and SAR data is proposed. Firstly, preliminary imaging is performed based on MEMS-IMU motion compensation data. The corner reflectors or strong target points based on site layout are used as the distinctive points of the image. SAR data uses phase history, Doppler information and Doppler frequency modulation to estimate platform relative motion error and attitude information in the original data domain and complex image domain [25], [26]. Then, analysis of motion error characteristics caused by random drift error of MEMS inertial navigation based on MEMS-IMU and SAR signal level data fusion method. The SAR-assisted MEMS-IMU random error drift model is constructed combining with the motion characteristics of the multi-rotor UAV platform. This model can be used to correct the long-term random drift of MEMS-IMU. Finally, the estimated state and measurement information of Kalman filtering can be determined based on motion error estimation results and fusion processing methods, and the state equation and measurement equation can also be constructed. The bidirectional smooth Kalman filtering processing would be finished combining with the original GPS/INS data. The filter processing result should be output to the SAR coherent imaging processing again. The above operating process should be repeatedly carried out until the motion estimation result is stable. In conclusion of the above method, ideal motion error compensation with a good focusing effect will be eventually achieved.

IV. RESULTS DISCUSSION

According to the above development of the SAR system program and the key technologies, the W-band UAV-based mini-SAR is exhibited in Fig. 11. All the antennas, RF components and digital circuits have been integrated into a small cube box. The top circuit layout integrates antennas and the millimeter wave front-end circuits. The middle layer integrates the LFM source and power circuits. And the bottom

FIGURE 12. W band mini-SAR prototype on a multi rotor UAV platform.

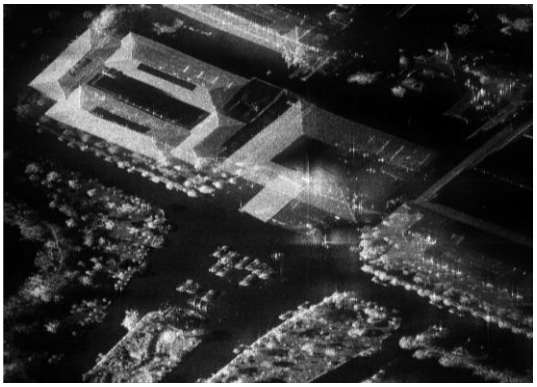

FIGURE 13. Imaging results of this developed W-band mini-SAR.

circuit wafer integrates the intermediate frequency and digital circuits. It is worth mentioning that the low-loss connection between antennas and millimeter-wave front-end is achieved by using the vertical transmission line interconnection technology. This SAR system prototype has the weight of 400 g, the volume of 67 mm $\times$ 60 mm $\times$ 50 mm, and the system power consumption of about 25 watts.

The imaging measurement of this W-band mini-SAR prototype on a multi rotor UAV platform is carried out outdoor, as shown in Figure 12. All the W-band SAR, power supply battery, inertial measurement unit (IMU), Global Positioning System(GPS) and digital recorder are installed on this Multi rotor UAV platform simultaneously. During the experiment, the cruising height is 300 m, the speed is 15 m/s, and the main-beam direction angle is 30° with reference to the ground. The SAR is working at the mode of the side-view strip map mode, and the strip image has a width of about 308 m. At the same time, the original receiving SAR data, IMU data and GPS data are obtained. The high-resolution SAR images can be subsequently obtained with experimental data processing by the ωK algorithm, as illustrated in Fig. 13. It is clearly that the imaging results of the targets including the cars, trees, roads and buildings are recognized easily. The optical image from the Google earth in the same area is also given in Figure 14. By comparing these two pictures, the details of the ground objects are clearly visible, which indicates

FIGURE 14. The optical image from the Google earth.

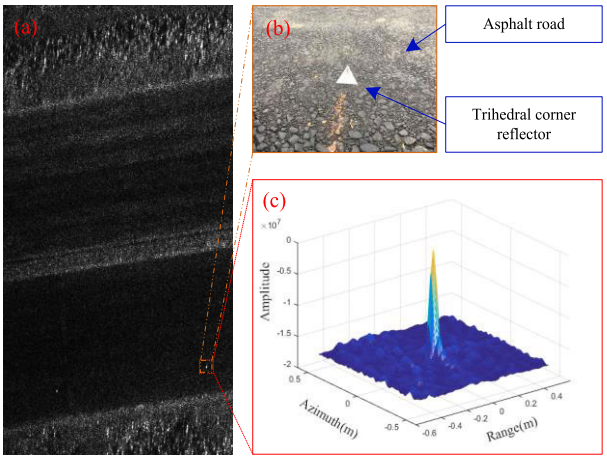

FIGURE 15. SAR image of asphalt road with trihedral corner reflectors. (a) SAR image. (b) Optical image of a trihedral corner reflector on asphalt road. (c) The Point Spread Function of the trihedral corner reflector plotted in 3-D.

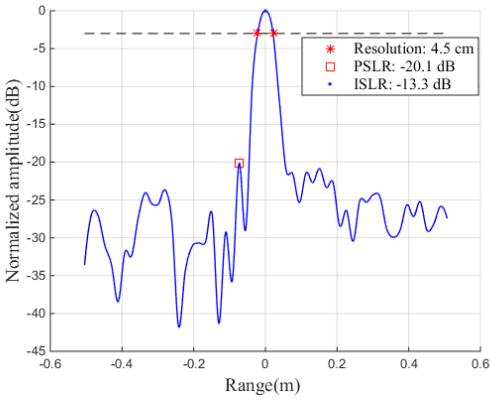

FIGURE 16. Range profile of the trihedral corner reflector.

that high resolution image quality has been achieved in this system.

In order to better evaluate the system performance, the response of a trihedral corner reflector are provided in Fig. 15. Its range and azimuth profiles are shown in Fig. 16 and Fig. 17, respectively. It can be concluded that,

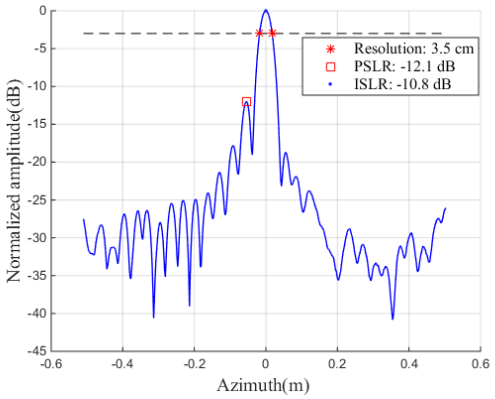

FIGURE 17. Azimuth profile of the trihedral corner reflector.

TABLE 2. Performance comparisons between the proposed SAR and the existing SARs.

Ref.	*System Name*	*Band*	*Resolution*	*Weight*
[28]	L-band SAR	L	0.75 m	~7.6 kg
[29]	microASAR	C	0.75 m	2.5 kg
[8]	ARBRES-X	X	1.5 m	2 kg
[30]	AMBER	X	0.1 m	6 kg
[31]	Ku-band SAR	Ku	0.25 m	6 kg
[32]	UAVSAR	Ka	0.5 m	4 kg
[33][34]	SUMATRA	W	0.15 m	~2.2 kg
This work	Mini-SAR	W	0.045 m	0.4 kg

the resolutions in the ground range and the azimuth are 4.5 cm and 3.5 cm. In addition, the Peak Side Lobe Ratio (PSLR) is −20.1 dB in the range direction and −12.1 dB in the azimuth direction, the Integral Side Lobe Ratio is −13.3 dB in the range direction and −10.8 dB in the azimuth respectively. Note that, compared to the theoretical performances (4.3 cm in the ground range, and 3.0 cm in the azimuth), there exists resolution degradations. The degradations are introduced by numerous systematical errors including the nonlinearity of the FM signal [27], the instability of UAV platform and the poor noise of PLL, *et al*. In particular, the multi-rotor UAV with large vibration of roll angle is vulnerable to the wind, even under the speed condition of 8 m/s. The unstable movements of the platform would introduce residual motion error leading to degradation of performance. However, the multi-rotor UAV has better flexibility. In our future work, the impact of this platform will be modeled, analyzed, and compensated.

Finally, a performance comparison between our developed system and the existing ones [8], [28]–[34] is provided in Table 2. From the perspective of resolution, volume, weight and power consumption, we can conclude that the proposed system has obvious advantages.

V. CONCLUSION

A W-Band 3-D integrated mini-SAR system with high imaging resolution on UAV platform has been discussed and presented in this paper. A series of methods such as the LFM wave generation technology based on analog PLL, high isolation millimeter-wave transceiver antennas based on EBG and the W-band motion compensation method based on the signal data fusion have been used to achieve the high imaging resolution. Furthermore, the 3D high-density integration process has been adopted to complete system miniaturization of about 400 g weight and 67 mm × 60 mm × 50 mm volume. The imaging resolution better than 4.5 cm and fine focusing effect have been demonstrated of this SAR system on the multi-rotor UAV platform. To the best of authors' knowledge, such mini-SAR with advantages of weight, volume, power consumption and state-of-the-art imaging resolution is developed in W band for the first time. Therefore, this UAV-based SAR will provide potential applications for high-accuracy remote sensing and differential tomography imaging. Such system design is promising to future research chip-level integrated SAR too.

REFERENCES

[1] J. Everaerts, "The use of unmanned aerial vehicles (UAVs) for remote sensing and mapping," *Int. Arch. Photogramm., Remote Sens. Spatial Inf. Sci.*, vol. 37, pp. 1187–1192, Jul. 2008.
[2] A. Moreira, P. Prats-iraola, M. Younis, G. Krieger, I. Hajnsek, and K. P. Papathanassiou, "A tutorial on synthetic aperture radar," *IEEE Geosci. Remote Sens. Mag.*, vol. 1, no. 1, pp. 6–43, Mar. 2013.
[3] G. Virone, A. M. Lingua, M. Piras, A. Cina, F. Perini, J. Monari, F. Paonessa, O. A. Peverini, G. Addamo, and R. Tascone, "Antenna pattern verification system based on a micro unmanned aerial vehicle (UAV)," *IEEE Antennas Wireless Propag. Lett.*, vol. 13, pp. 169–172, Jan. 2014.
[4] A. Bhardwaj, L. Sam, H. Akansha, F. J. Martín-Torres, and R. Kumar, "UAVs as remote sensing platform in glaciology: Present applications and future prospects," *Remote Sens. Environ.*, vol. 175, pp. 196–204, Mar. 2016.
[5] S. Jung, H. Cho, D. Kim, K. Kim, J.-I. Han, and H. Myung, "Development of algal Bloom removal system using unmanned aerial vehicle and surface vehicle," *IEEE Access*, vol. 5, pp. 22166–22176, 2017.
[6] M. G. Fernandez, Y. A. Lopez, A. A. Arboleya, B. G. Valdes, Y. R. Vaqueiro, F. L.-H. Andres, and A. P. Garcia, "Synthetic aperture radar imaging system for landmine detection using a ground penetrating radar on board a unmanned aerial vehicle," *IEEE Access*, vol. 6, pp. 45100–45112, 2018.
[7] A. Aguasca, R. Acevo-Herrera, A. Broquetas, J. Mallorqui, and X. Fabregas, "ARBRES: Light-weight CW/FM SAR sensors for small UAVs," *Sensors*, vol. 13, no. 3, pp. 3204–3216, Mar. 2013.
[8] M. Lort, A. Aguasca, C. Lopez-Martinez, and T. M. Marin, "Initial evaluation of SAR capabilities in UAV multicopter platforms," *IEEE J. Sel. Topics Appl. Earth Observ. Remote Sens.*, vol. 11, no. 1, pp. 127–140, Jan. 2018.
[9] D. M. Sheen, D. L. Mcmakin, and T. E. Hall, "Three-dimensional millimeter-wave imaging for concealed weapon detection," *IEEE Trans. Microw. Theory Techn.*, vol. 49, no. 9, pp. 1581–1592, Sep. 2001.
[10] S. Hantscher, B. Schlenther, M. Hagelen, S. A. Lang, H. Essen, A. Tessmann, A. Hulsmann, A. Leuther, and M. Schlechtweg, "Security pre-screening of moving persons using a rotating multichannel *W*-band radar," *IEEE Trans. Microw. Theory Techn.*, vol. 60, no. 3, pp. 870–880, Mar. 2012.
[11] H. Wang, Y. Xia, M. Jiang, and L. Kong, "Research on W-band FMCW rail-SAR system with high resolution," in *Proc. 18th Int. Radar Symp. (IRS)*, Jun. 2017, pp. 1–6.
[12] T.-Y. Lee, V. Skvortsov, M.-S. Kim, S.-H. Han, and M.-H. Ka, "Application of *W*-band FMCW radar for road curvature estimation in poor visibility conditions," *IEEE Sensors J.*, vol. 18, no. 13, pp. 5300–5312, Jul. 2018.

[13] S.-Y. Jeon, M.-H. Ka, S. Shin, M. Kim, S. Kim, S. Kim, J. Kim, A. Dewantari, J. Kim, and H. Chung, "W-band MIMO FMCW radar system with simultaneous transmission of orthogonal waveforms for high-resolution imaging," *IEEE Trans. Microw. Theory Techn.*, vol. 66, no. 11, pp. 5051–5064, Nov. 2018.
[14] S.-Y. Jeon, S. Kim, J. Kim, S. Kim, S. Shin, M. Kim, and M.-H. Ka, "W-band FMCW MIMO radar system for high-resolution multimode imaging with time- and frequency-division multiplexing," *IEEE Trans. Geosci. Remote Sens.*, early access, Feb. 20, 2020, doi: 10.1109/TGRS.2020.2971998.
[15] M. Ding, L. Xingdong, T. Li, W. Zhilei, and W. Yixiao, "Design and verification of monolithic integrated SAR system," *J. Electron. Inf. Technol.*, vol. 40, no. 11, pp. 2645–2650, 2018.
[16] P.-J. Peng, P.-N. Chen, C. Kao, Y.-L. Chen, and J. Lee, "A 94 GHz 3D image radar engine with 4TX/4RX beamforming scan technique in 65 nm CMOS technology," *IEEE J. Solid-State Circuits*, vol. 50, no. 3, pp. 656–668, Mar. 2015.
[17] B. Cheng, G. Jiang, C. Wang, C. Yang, Y. Cai, Q. Chen, X. Huang, G. Zeng, J. Jiang, X. Deng, and J. Zhang, "Real-time imaging with a 140 GHz inverse synthetic aperture radar," *IEEE Trans. THz Sci. Technol.*, vol. 3, no. 5, pp. 594–605, Sep. 2013.
[18] M. Ding, X. Liang, L. Tang, Z. Wen, X. Wang, and Y. Wang, "Micro FMCW SAR with high resolution for mini UAV," in *Proc. Int. Conf. Microw. Millim. Wave Technol. (ICMMT)*, May 2018, pp. 1–3.
[19] M. Ding, L. Tang, L. Zhou, X. Wang, Z. Weng, and J. Qu, "W band mini-SAR on multi rotor UAV platform," in *Proc. IEEE 2nd Int. Conf. Electron. Inf. Commun. Technol. (ICEICT)*, Jan. 2019, pp. 416–418.
[20] Z. Zhao, "New progress of the micro system three-dimensional integration technology," *Micronanoelectron. Technol.*, vol. 54, no. 1, pp. 1–10, Jan. 2017.
[21] Y. Li and D. Goyal, *3D Microelectronic Packaging: From Fundamentals to Applications*. Berlin, Germany: Springer, 2017.
[22] J. Hao and W. Xiang, "3D Heterogeneous integration for micro-system and its application," *Electron. Process Tech.*, vol. 39, no. 6, pp. 317–321, Nov. 2018.
[23] Y. Zhang, R. Zhang, J. Zhang, T. Bai, A. F. Al Rawi, M. Moonen, and L. Hanzo, "Far-end crosstalk mitigation for future wireline networks beyond G.mgfast: A survey and an outlook," *IEEE Access*, vol. 8, pp. 9998–10039, 2020.
[24] J.-Y. Lee, S.-H. Kim, and J.-H. Jang, "Reduction of mutual coupling in planar multiple antenna by using 1-D EBG and SRR structures," *IEEE Trans. Antennas Propag.*, vol. 63, no. 9, pp. 4194–4198, Sep. 2015.
[25] B. Fan, Z. Ding, W. Gao, and T. Long, "An improved motion compensation method for high resolution UAV SAR imaging," *Sci. China Inf. Sci.*, vol. 57, no. 12, pp. 1–13, Dec. 2014.
[26] W. Xu, B. Wang, M. Xiang, L. Zhou, X. Fu, and S. Wang, "A frequency-phase gradient autofocus algorithm for excessive migration in UAV SAR images," in *Proc. 6th Asia–Pacific Conf. Synth. Aperture Radar (APSAR)*, Nov. 2019, pp. 11–16.
[27] P. V. Brennan, Y. Huang, M. Ash, and K. Chetty, "Determination of sweep linearity requirements in FMCW radar systems based on simple voltage-controlled oscillator sources," *IEEE Trans. Aerosp. Electron. Syst.*, vol. 47, no. 3, pp. 1594–1604, Jul. 2011.
[28] O. Frey, C. L. Werner, and R. Coscione, "Car-borne and UAV-borne mobile mapping of surface displacements with a compact repeat-pass interferometric SAR system at L-band," in *Proc. IEEE Int. Geosci. Remote Sens. Symp. (IGARSS)*, Jul. 2019, pp. 274–277.
[29] E. Zaugg, M. Edwards, D. Long, and C. Stringham, "Developments in compact high-performance synthetic aperture radar systems for use on small unmanned aircraft," in *Proc. Aerosp. Conf.*, Mar. 2011, pp. 1–14.
[30] M. W. van der Graaf, M. P. G. Otten, A. G. Huizing, R. G. Tan, M. C. Cuenca, and M. G. A. Ruizenaar, "AMBER: An X-band FMCW digital beam forming synthetic aperture radar for a tactical UAV," in *Proc. IEEE Int. Symp. Phased Array Syst. Technol.*, Oct. 2013, pp. 165–170.
[31] W. X. Liu, H. C. Feng, S. Y. Aye, B. P. Ng, and Y. L. Lu, "Design and testing of multi-rotor UAV full-pol SAR system," in *Proc. Int. Conf. Radar Syst. (Radar)*, 2017, pp. 1–5.
[32] M. Edrich and G. Weiss, "Second-generation ka-band UAV SAR system," in *Proc. 38th Eur. Microw. Conf.*, Oct. 2008, pp. 479–482.
[33] H. Essen, M. Bräutigam, R. Sommer, A. Wahlen, W. Johannes, J. Wilcke, M. Schlechtweg, and A. Tessmann, "SUMATRA, a W-band SAR for UAV application," in *Proc. Int. Radar Conf.*, 2019, pp. 1–4.
[34] H. Essen, W. Johannes, S. Stanko, R. Sommer, A. Wahlen, and J. Wilcke, "High resolution W-band UAV SAR," in *Proc. IEEE Int. Geosci. Remote Sens. Symp.*, Jul. 2012, pp. 5033–5036.

MAN-LAI DING was born in Shanxi, China, in 1982. He received the M.S. degree in electromagnetic field technology from the University of Electronic Science and Technology of China, Chengdu, China, in 2010, and the Ph.D. degree in signal processing technology from the University of Chinese Academy of Sciences, Beijing, China, in 2018.

He is currently an Assistant Researcher with the Aerospace Information Research Institute, Chinese Academy of Sciences, Beijing. His research interests include design of imaging radar systems and radar signal processing.

CHI-BIAO DING received the B.S. and Ph.D. degrees in electronics engineering from Beihang University, Beijing, China, in 1997.

Since 1997, he has been with the Aerospace Information Research Institute, Chinese Academy of Sciences, Beijing, where he is currently a Research Fellow and the Vice Director. His research interests include advanced synthetic aperture radar systems, signal processing technology, and information systems.

LI TANG was born in Sichuan, China, in 1988. He received the master's degree in electromagnetic field and microwave technology from the Beijing Institute of Technology, China, in 2013.

He is currently an Assistant Researcher with the Aerospace Information Research Institute, Chinese Academy of Sciences, Beijing, China. His research interests include chip-based radar micro-systems and miniature synthetic aperture radars.

XUE-MEI WANG was born in Inner Mongolia, China, in 1988. She received the master's degree in electronic communication engineering from Beihang University, Beijing, China, in 2014.

She is currently an Engineer with the Aerospace Information Research Institute, Chinese Academy of Sciences, China. Her research interests include design of miniaturized antenna with high-performance, phased-array antenna, and meta-material antenna.

JIA-MENG QU was born in Hebei, China, in 1992. She received the master's degree in microelectronics and solid-state electronics from Peking University, in 2017.

She is currently with the Aerospace Information Research Institute, Chinese Academy of Sciences, Beijing, China, as an Assistant Researcher. Her main research interests include chip radar and micro radar.

RUI WU received the B.S. and M.S. degrees from the University of Electronic Science and Technology of China, Chengdu, China, in 2006 and 2009, respectively, and the Ph.D. degree from the Tokyo Institute of Technology, Tokyo, Japan, in 2015.

From 2015 to 2018, he was a Postdoctoral Researcher with the Tokyo Institute of Technology. Since 2018, he has been a Full Professor with the National Key Laboratory of Microwave Imaging Technology, Aerospace Information Research Institute, Chinese Academy of Sciences, Beijing, China. His current research interests include RF/millimeter-wave transceivers for radar and high-data rate wireless communications.